

Received January 22, 2019, accepted February 9, 2019, date of publication February 15, 2019, date of current version March 5, 2019.

Digital Object Identifier 10.1109/ACCESS.2019.2899650

An Improved Position Determination Algorithm Based on Nonlinear Compensation for Ground-Based Positioning Systems

JINGXUAN SU, ZHENG YAO^{ID}, AND MINGQUAN LU

Department of Electronic Engineering, Tsinghua University, Beijing 100084, China

Corresponding author: Zheng Yao (yaozheng@tsinghua.edu.cn)

This work was supported by the National Natural Science Foundation of China under Grant 61771272.

ABSTRACT In the absence of GNSS or when signals from satellites are blocked in harsh environments, a ground-based positioning system can be used to estimate the position of users and receivers. Nevertheless, ground-based systems suffer dramatic nonlinear error resulting from the linearization used in typical positioning algorithms. Robust positioning algorithms that are capable of handling strong nonlinearity cases are therefore of great value. In this paper, we propose an algorithm termed promoted iterative least-squares based on nonlinear-compensation (PILSBON) to effectively alleviate the influence of nonlinear effects. This algorithm is based on the accurate expression of the nonlinear error terms in the double-differenced pseudorange measurement model. In order to eliminate the effects of nonlinearity for targeted solutions, the PILSBON uses iterative numerical estimation to compensate for nonlinear error so that the nonlinear position determination is transformed into a linear model, which can then be estimated with a linear estimation algorithm. In this paper, we analyze the properties of the PILSBON and compare it to conventional solutions. Because of its specific strategy for nonlinearity, our results show that the PILSBON improves the overall accuracy by approximately 30% compared with conventional solutions according to statistic RMSE data from over 500 experiments and positions. Moreover, by deploying a practical ground-based positioning system with six transmitters on the rooftop of our laboratory building, we demonstrate that the PILSBON algorithm can be efficiently employed in real-world experiments.

INDEX TERMS Nonlinear compensation, ground-based positioning system, positioning algorithm, differential pseudorange, least-squares estimation.

I. INTRODUCTION

The world is becoming more and more reliant on GNSS positioning services which are now used in many different devices. However, due to the weakness of received signal strength caused by the working environment, the performance of GNSS decreases in harsh environments such as open-pit mines, urban canyons, ports or the battlefield with strong electromagnetic interference [1].

As an alternative, positioning systems based on ground-based transmitters and the same principles as GNSS are employed with the potential of achieving positioning results to centimeter-level [3]. The advantage of getting rid of the ionosphere effect and being easy to be deployed bring outstanding adaptability and universality [2], [4]–[6], [8].

The associate editor coordinating the review of this manuscript and approving it for publication was Venkata Ratnam Devanaboyina.

As a result of great potential, various techniques, such as ultra-tight integration [30], differential measurements [4], precise point positioning (PPP) [7] and carrier phase positioning, are have been studied for further improvement on accuracy and robustness [5]–[8], [11], [18]. However, former studies failed to make ground-based systems perfectly applied due to several essential drawbacks, one of which is the nonlinearity [20]. The obvious effect of nonlinear error makes it impossible to simply use positioning principles of GNSS, such as linearization and least-squares estimation [2], [8]. Additionally, the overall positioning performance will be limited more by nonlinearity within the narrower field. Therefore, more special techniques should be considered for further improvement.

In order to resolve the nonlinear errors mentioned, many solutions have been proposed. The main strategy used in the proposed algorithms is mainly the use of robust

numerical methods to improve the overall ability to alleviate the nonlinearity. The first bunch of algorithms concentrates on code pseudorange applications, such as the Levenberg-Marquardt (LM) method [16], [17], which uses a specific parameter to control the iterative length to interpolate between the Gauss-Newton algorithm [9] and the method of gradient descent. In other words, there are complicated portions in traditional algorithms, like step-limiting iterative procedures, to make sure the positioning results to diverge effectively based on robust calculation. While these methods that pursue robustness by sacrificing the algorithm's efficiency can be alternated by some masterly design.

The second type of methods focuses on positioning applications based on carrier phase information, which provides the potential of centimeter-level positioning accuracy [6]. Due to the inevitable existence of nonlinear error, it is necessary to adopt the universal nonlinear numerical estimation method, such as the LM algorithm previously mentioned, or to apply nonlinear methods for carrier-phase positioning specifically [21]–[23]. Many related algorithms such as Particle Swarm Optimizations (PSO) [11] and Unscented Kalman Filter (UKF) algorithm [10] have been proposed. However initial estimation is required for most conventional nonlinear methods for the carrier's whole-circumference ambiguity. For example, the PSO method and UKF method employed in the indoor positioning systems usually request an initial estimation within a limited error (usually no more than twenty centimeters) [11].

Besides these two aspects, there are other latest integration algorithms used for nonlinearity scenarios. For example the combination between ground-based systems and Pedestrian Dead Reckoning (PDR), which calls for extra devices attached with receivers [28]. Besides, the principle optimal dilution of precision and weighting adjustment with multiple array transmitters are also combined and considered for the robustness of positioning, which should be achieved based on multiple redundant devices [29]. Therefore it is necessary to develop a positioning algorithm which is capable of resolving the nonlinear effect and achieving position determination easily without a reliable initial estimation.

In view of the shortcomings of the algorithms mentioned above, we propose an algorithm named PILSBON based on a specific principle named nonlinear compensation in this paper. The numerical expression of the nonlinear compensation is derived referring to the differential code pseudorange model and the geometric distribution of transmitters in ground-based systems. By adding the special compensation, the nonlinear error coming from the loss of the high-order remainders of the Taylor expansion is removed throughout the iterative estimation process. The advantages of the algorithm over the conventional algorithms previously discussed are twofold. First, when pseudorange is used as the observation, an precise positioning solution can be independently performed at each epoch with the absence of accurate initial estimations. Second, the position determination can be proceeded by the most basic numerical estimation algorithm,

such as linear least-squares, with the compensation. The core idea behind this algorithm is improving the efficiency of the method based on a specific applied scenario, where some a priori knowledge of the positioning problem itself can be considered to obtain the solution obtained more carefully. Furthermore, the unknown parameter in the proposed algorithm is related to the measurements with a linear form, the nonlinearity is solved essentially.

In this paper, we perform a statistical analysis of the proposed algorithm to prove that the algorithm can reduce the nonlinear effect. We then confirm that this improves position determination accuracy through experiments. The simulations demonstrate the feasibility of the proposed algorithm in strong nonlinear scenarios. Based on that, experiments based on a practical ground-based positioning system deployed on the rooftop of our laboratory were carried out. When designing the simulation and experiment, the differential positioning systems are considered. Additionally, two specific application scenarios are considered, one where the position of the reference receiver in the double-differenced measurement model is unknown and the other where it is known. These two scenarios are termed relative positioning and absolute positioning respectively.

The remaining sections of this paper are organized as follows. First, the observation model in ground-based positioning systems and the related nonlinear error-based algorithm is presented in Section II. Second, the principles of nonlinear compensation and procedures of the PILSBON algorithm are detailed in Section III. Third, both simulations and experimental results of the PILSBON algorithm are shown and analyzed in Section IV. Finally, we present our conclusions in Section V.

II. OBSERVATION MODEL AND NONLINEAR ERROR

Both GNSS and ground-based positioning system based on transmitters and receivers have a universal observation model and positioning principles in position determination systems. This section will discuss the differences in transmitter definition, followed by the linearization process and the resulted nonlinear error [2], [19].

A. OBSERVATION MODEL

Distance is defined by TOA within the positioning systems based on transmitters and receivers and is known as the pseudorange observed. The observation equation for pseudorange from transmitters is tracked by receiver r at epoch t , written as

$$p_r^s(t) = \rho_r^s(t, t - \tau_r^s) + cd t_r(t) - cd t^s(t - \tau_r^s) + T_r^s(t) + e_r^s(t). \quad (1)$$

The meaning of notation in (1) is as follows: p_r^s and ρ_r^s present respectively the pseudorange observation and real receiver-transmitter range, τ_r^s shows the travel time of the signal and the velocity of light is written as c . For error terms; receiver clock error is written as dt_r .

For transmitter-related terms; the clock error is shown by dt^s , similar to receiver-related errors. In addition, the effect caused by the transmission process is written as T_r^s , which means the ionospheric and tropospheric effect in GNSS. As for random code noise, it is shown as e_r^s .

The observation equation (1) will be used in remaining sections of this paper, therefore the meaning of notations will not be repeated.

B. LINEARIZATION IN POSITIONING ALGORITHMS

Linearization, where higher-order remainders are eliminated, is the source of nonlinear error, both in single-point or differenced positioning [2]. In some terrestrial positioning systems with high requirements on positioning accuracy, the usage of the differential mechanism can mitigate the influence of such device-related errors and maximize the positioning performance of the system. As a widely used signal model, the differential technique is explained in detail in the related literature [19].

1) LINEARIZATION IN SINGLE-POINT POSITIONING MODEL

The linearization process of the traditional positioning algorithm has been well known, very detailed reasoning and explanation of which can be found in [19]. The incremental receiver-transmitter range $\Delta\rho_r^s(t, t - \tau_r^s)$ in the linearization formula is computed as follows.

$$\Delta\rho_r^s(t, t - \tau_r^s) = -[e_{r_0}^s(t)]^T \cdot \Delta r_r(t) - \dot{\rho}_{r_0}^s(t) \Delta dt_r(t) \tag{2}$$

where $e_{r_0}^s(t)$ denotes the Line of Sight (LOS) vector from the transmitter to the estimated position of the receiver and $\dot{\rho}_{r_0}^s(t)$ means the first derivative of the pseudorange on the receiver clock bias. Furthermore, $\Delta r_r = r_r - r_{r_0}$ is defined as the error of the estimated receiver position.

According to the above equations, the final error equation can be obtained. Equation (3) denotes the error function corresponding to each transmitter. The Jacobian matrix J_0 for the nonlinear least-squares estimation is defined in

$$E \left(\begin{matrix} \Delta\hat{\rho}_r^1 \\ \vdots \\ \Delta\hat{\rho}_r^m \\ \Delta\hat{\rho}_r^s(t) \end{matrix} \right) = \underbrace{\begin{bmatrix} -[e_r^1(t)]^T & 1 \\ \vdots & \vdots \\ -[e_r^m(t)]^T & 1 \end{bmatrix}}_{J_0} \begin{bmatrix} \Delta r_r(t) \\ c\Delta dt_r(t) \end{bmatrix} \tag{3}$$

where $E(\cdot)$ denotes the expectation on parameters within the bracket, while $\hat{\rho}_r^s(t)$ defines the pseudorange which has been corrected for transmission errors. The m denotes the number of transmitters. The $\dot{\rho}_{r_0}^s(t)$ in (2) should have appeared in (3), however, is eliminated because of the clock bias. The effect of the receiver clock bias on pseudorange is defined as $c\Delta dt_r(t)$, which should be combined with the $\dot{\rho}_{r_0}^s(t)$ and written as $(c - \dot{\rho}_{r_0}^s(t)) \Delta dt_r(t)$. Nevertheless, the $\dot{\rho}_{r_0}^s(t)$ has the same magnitude with the velocity of the receiver with

respect to the transmitter, which is much less than the speed of light, so that is eliminated in (3). To be more compactly, the Jacobian matrix is written as

$$J_0 = [G_r^s(t), u_{ms}] \tag{4}$$

where $G_r^s(t) = [-[e_r^1(t)]^T, \dots, -[e_r^m(t)]^T]^T$ and $u_{ms} = \underbrace{[1, \dots, 1]}_m^T$. These formulas and parameters will be used below in following sections.

2) LINEARIZATION IN DIFFERENTIAL POSITIONING MODEL

In the proposed algorithm, the double-differenced measurement is used for both simulations and experiments in this paper. The linearization formula of that is shown here.

The double-differenced model is mainly divided into two parts in the proposed algorithm. One is the between-receiver single differenced positioning, with a position-known reference receiver selected as $r = 1$. The other is the between-transmitter single differenced positioning with a chosen pivot transmitter p from all transmitters [5].

The double-differenced observation model is applied and shown as $D_m^T \Delta\tilde{p}_r^s(t)$. The differencing matrix

$$D_m^T = \begin{bmatrix} I_{p-1} & -u_{p-1} & 0 \\ 0 & -u_{m-p} & I_{m-p} \end{bmatrix} \tag{5}$$

is formed depending on the pivot transmitter chosen according to the geographic distribution of visible transmitters.

The corresponding error equation of linearization obtained is presented as (6).

$$E \left(D_m^T \Delta\tilde{p}_r^s(t) \right) = \underbrace{\begin{bmatrix} D_m^T G_r(t) \\ J_0 \end{bmatrix}}_{J_0} \Delta\tilde{x}_r(t) \tag{6}$$

where $\tilde{p}_r^s(t) = [\tilde{p}_r^1(t), \dots, \tilde{p}_r^m(t)]^T$ represents the differenced pseudorange observation between the receiver and the reference receiver.

The unknown parameter $\tilde{x}_r(t)$ is defined as the coordinates of the vector between receiver r and reference receiver 1, defined as $\tilde{x}_r(t) = r_1(t) - r_r(t)$. Thus the $\Delta\tilde{x}_r(t)$ is defined as $\Delta\tilde{x}_r(t) = \tilde{x}_r(t) - \tilde{x}_{r_0}(t)$.

Based on the linearization process of the double-differenced pseudorange model, the derivation of nonlinear error is explained in the next section.

C. NONLINEAR ERROR

The linear approximation results in a nonlinearity error in the measurements model.

It is derived in former works [2], [8], [20] that the nonlinear error is caused by eliminating the second-order and higher-order remainders in the linearization process and has the upper and lower bounds described in (7).

$$\frac{1}{2} \lambda_{\min} \|r_r - r_{r_0}\|^2 \leq R \leq \frac{1}{2} \lambda_{\max} \|r_r - r_{r_0}\|^2 \tag{7}$$

where R denotes the second-order remainder of the expansion, λ_{\min} and λ_{\max} represent the minimum and maximum eigenvalues of the Hessian matrix $H(\theta)$.

The extreme eigenvalues of the Hessian matrix in the position determination are $\lambda_{\min} = 0$ and $\lambda_{\max} = 1/\rho_r^s$. Thus the (7) is written as

$$0 \leq R \leq \frac{1}{2} \frac{\Delta r_r}{\rho_r^s} \quad (8)$$

Therefore, the linearization error bound varies with the change in pseudorange and the initial error of estimation.

According to (7), the nonlinear error will be close to zero and ignored in GNSS applications, which is different from the ground-based transmitter systems.

When the separation between ground-based transmitter and receiver is 200 m, which corresponds to ρ_r^s of 200m, an error of 15m in coordinates, in reference to Δr_r , may result in a linearization error of as much as 0.6 m [10].

Corresponding to the differenced positioning model, the bound of the nonlinear error is derived as follows. It is obvious that the bounds of the nonlinear error change for a different transmitter. The bound values in double-difference positioning are shown in (9).

$$0 \leq R_d \leq \max \left(\frac{1}{2} \frac{\Delta r_r}{\rho_r^s}, \frac{1}{2} \frac{\Delta r_r}{\rho_r^p} \right) \quad (9)$$

where R_d denotes the nonlinear error of the differenced measurement model, which is written as $R_d = R^s - R^p$. The superscript s and p denote the corresponding transmitter. The ρ_r^s and ρ_r^p denotes the pseudorange between the receiver and a transmitter s and the pivot transmitter p respectively.

In the next Section, the specific nonlinear compensation and the PILSBON algorithm based on it are proposed to overcome the nonlinear effect in ground-based positioning systems.

III. NONLINEAR COMPENSATION AND PROPOSED ALGORITHM

In this Section, the principle of nonlinear compensation for solving potential decline due to nonlinear error is first presented. Next, the PILSBON algorithm based on it is described. The nonlinear compensation proposed here is in the scenarios of ground-based positioning systems in the following sections of this paper.

A. NONLINEAR COMPENSATION

With sufficient knowledge of the resource of the nonlinear error, the error can be removed more essentially according to the last section.

The nonlinear compensation discussed herein achieves another decomposition model of the differenced pseudorange measurements and is used to alleviate the effect of nonlinear error in a ground-based positioning system.

In order to clearly show the derivation of the nonlinear compensation, both the nonlinear compensation in the single differenced positioning and double-differenced positioning model are derived.

1) NONLINEAR COMPENSATION IN THE SINGLE-DIFFERENCED POSITIONING

In the single differenced positioning, derivation of the nonlinear compensation is carried for convenience and clearness.

Unlike the traditional linearization process in the typical between-receiver positioning model, we rewrite the differenced pseudorange as a new form in (10)

$$\rho_{1r}^s(t) = \tilde{x}_r(t)^T \cdot e_r^s(t) - \rho_1^s(t) \left(1 - e_1^s(t)^T \cdot e_r^s(t) \right) \quad (10)$$

where $\rho_{1r}^s(t) = \rho_r^s(t) - \rho_1^s(t)$.

The single-differenced pseudorange is composed of two parts without any approximation. The first part in (10) can be regarded as the combination of the zero-order and the first-order terms of the expansion. The second part can be regarded as a compensation term which denotes the higher-order remainders which is precisely the nonlinear compensation proposed in this paper.

The numerical expression of the compensation is defined as

$$\varepsilon_n = \rho_1^s(t) \cdot \left(1 - e_1^s(t)^T \cdot e_r^s(t) \right) \quad (11)$$

So that the observation error function can be further organized as

$$\Delta \tilde{\rho}_r^s(t) = (p_r^s(t) - p_1^s(t)) - \tilde{x}_r(t)^T \cdot e_r^s(t) + \varepsilon_n \quad (12)$$

Since the position of both the reference receiver and transmitters are already known by survey techniques, the estimation is only affected by the change on $\tilde{x}_r(t)$, which is the unknown parameter in the PILSBON algorithm.

The analysis of the above pseudorange decomposition is implemented referring to the methodology in [4, Sec. 3.1]. The definition of nonlinear compensation is better illustrated by a schematic diagram.

Considering the application context in a ground-based positioning system, the magnitude of nonlinear error changes a lot because of the decrease in the distance between transmitters and the receiver [3], [4]. The estimation procedure and the existence of nonlinear compensation can be presented in Fig. 1.

In Fig. 1, the gap between $\rho_r^s(t) - \rho_1^s(t)$ and $\tilde{x}_r(t)^T \cdot e_r^s(t)$ is exactly the nonlinear error affecting the positioning process. The physical meaning of nonlinear error ε_n is the discrepancy between ρ_1^s and its projection on $e_r^s(t)$.

Correspondingly, the $(\tilde{x}_r(t) + \delta \tilde{x}_r(t))^T \cdot e_{r_0}^s(t)$ cannot be used to approximate the $\rho_{r_0}^s(t) - \rho_1^s(t)$ in the iterative estimation process.

With the application of nonlinear compensation, however, the $\tilde{x}_r(t)^T \cdot e_r^s(t)$ can be used to approximate $\rho_r^s(t) - \rho_1^s(t)$ by adding the nonlinear compensation ε_n up, which is derived from the estimated position r_0 . The relation between the unknown parameters $\tilde{x}_r(t)$ and the differenced pseudorange $\rho_r^s(t) - \rho_1^s(t)$ is then linear. As a result, the conventional linear least-squares estimation can be used with the help of the compensation.

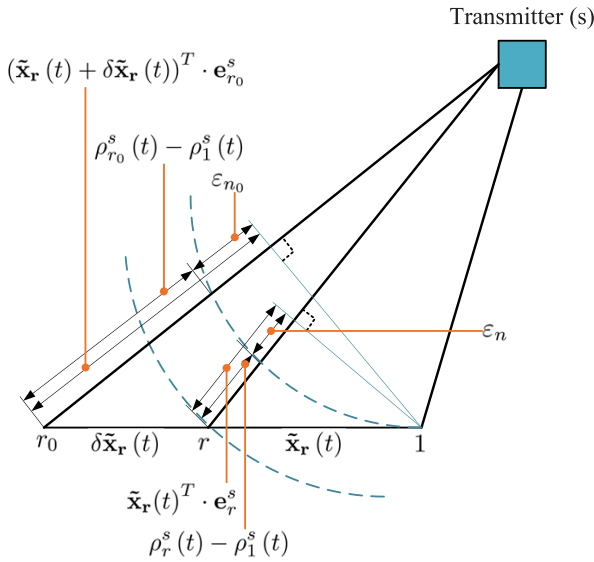


FIGURE 1. Estimation of the unknown parameter in ground-based positioning systems and definition of the nonlinear error in the single-differenced model.

2) NONLINEAR COMPENSATION IN THE DOUBLE-DIFFERENCED POSITIONING

As in Section III.A.1, the significance of the nonlinear compensation in double-differenced positioning is shown using a schematic diagram corresponding to this model in Fig. 2.

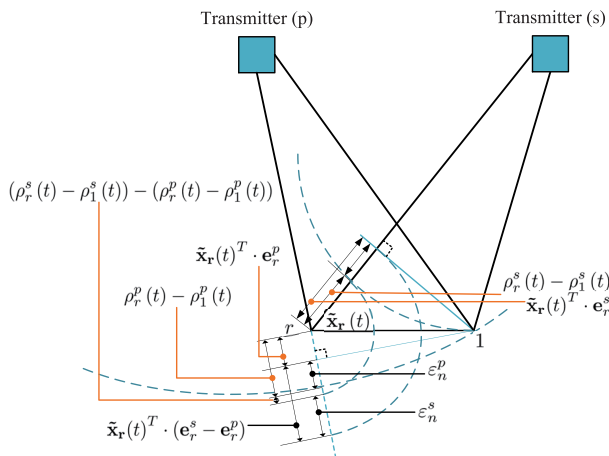


FIGURE 2. Estimation of the unknown parameter in ground-based positioning systems and definition of the nonlinear error in the double-differenced positioning model.

Same as what is derived from the single-differenced case in Fig. 1, the nonlinearity-related approximation problem also exists in the double difference. It is shown in Fig. 2 that there is a gap between the double-differenced

pseudorange $(\rho_r^s(t) - \rho_1^s(t)) - (\rho_r^p(t) - \rho_1^p(t))$ and the $\tilde{x}_r(t)^T \cdot (e_r^s(t) - e_r^p(t))$, like the scenario in Fig. 1. The gap can be calculated precisely with the combination of nonlinear compensation ε_n^s and ε_n^p where ε_n^s and ε_n^p denote the compensation related to transmitter s and p respectively. Thus the double-differenced pseudorange $(\rho_r^s(t) - \rho_1^s(t)) - (\rho_r^p(t) - \rho_1^p(t))$ can be written as a linear form as (13), as shown at the bottom of this page.

Referring to the (6), the error equation for the double difference model can be obtained. The error function is written as

$$D_m^T \cdot \Delta \tilde{p}_r^s(t) = D_m^T \cdot \begin{bmatrix} p_r^1(t) - p_1^1(t) \\ \vdots \\ p_r^m(t) - p_1^m(t) \end{bmatrix} - [D_m^T \cdot G_r(t) I_{m-1}] \cdot \begin{bmatrix} \tilde{x}_r(t) \\ D_m^T \cdot \varepsilon_n(t) \end{bmatrix} \quad (14)$$

where ε_n is denoted as

$$\varepsilon_n(t) = \begin{bmatrix} \rho_1^1(t) \cdot (1 - e_1^1(t)^T \cdot e_1^1(t)) \\ \vdots \\ \rho_1^m(t) \cdot (1 - e_1^m(t)^T \cdot e_1^m(t)) \end{bmatrix} \quad (15)$$

and $\tilde{p}_r^s(t)$ is denoted as $\tilde{p}_r^s(t) = \begin{bmatrix} p_r^1(t) - p_1^1(t) \\ \vdots \\ p_r^m(t) - p_1^m(t) \end{bmatrix}$. The corresponding nonlinear compensation term is written as $D_m^T \cdot \varepsilon_n(t)$ for all transmitters.

The linear relationship between measurements and the unknown parameters, which can be estimated with least-squares, existing in the double-differenced positioning is written as (16), shown at the bottom of the next page.

Reviewing the differenced positioning model in (16), as shown at the bottom of the next page, the only unknown parameter is the relative position vector, which is the same as the unknown parameter in the between-receiver single differenced positioning. Furthermore, two terms should be estimated according to the current estimation of \tilde{x}_r , namely the matrix of the unit LOS vector $G_r(t)$ and nonlinear compensation ε_n . The last term in (16), the e_{dd} , denotes the synthesis of all potential error terms in the positioning problem. The relation between the differenced pseudorange measurements and the estimated unknown parameters is well clarified in (16).

To recapitulate, the nonlinear compensation referring to the higher-order remainders of the Taylor expansion is derived detailedly in this section. It shows that it is not always necessary to eliminate the remainders to achieve the linearized approximation. Based on the compensation, the PILSBON algorithm is presented in the next section.

$$(\rho_r^s(t) - \rho_1^s(t)) - (\rho_r^p(t) - \rho_1^p(t)) = [e_r^s(t) - e_r^p(t) \ 1] \begin{bmatrix} \tilde{x}_r(t) \\ \varepsilon_n^p - \varepsilon_n^s \end{bmatrix} \quad (13)$$

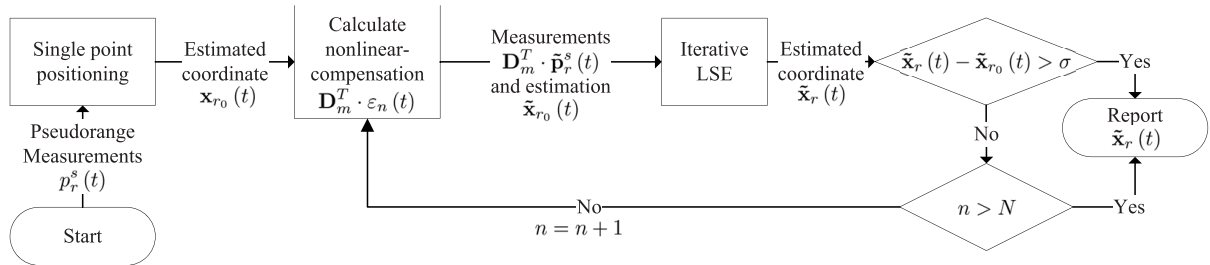


FIGURE 3. Flow chart of PILSBON algorithm, showing the calculation steps of every epoch.

B. PROPOSED ALGORITHM

1) ALGORITHM STEPS

The algorithm proposed is termed the Promoted Iterative Least-Squares Based on Nonlinear-compensation (PILSBON).

The algorithm is applied in a double-differenced model referring to the specific position of transmitters and reference receiver. There are three main steps included in the algorithm, namely initialization, estimation and update.

The algorithm proceeds iteratively. For the initialization step, a single-point solution is first carried out to obtain an estimated position as the initial estimation of the unknown parameter. For the estimation step, the LOS vector together with the nonlinear compensation is then calculated according to the latest position estimation. So far, all the necessary terms in (16) are available to accomplish the position determination by using the linear least-squares method. As for the update step, the update of the receiver position can be achieved iteratively as a conventional least-squares estimation, where the discrepancy between the latest two estimations is regarded as the terminal condition of iteration.

The specific steps of the algorithm are detailed as follows.

Step 1 (INITIALIZATION): Identify an initial estimation of position, select a pivot transmitter (chosed the main station or transmitter with the highest elevation angle to form the differencing matrix) and a reference receiver (position $x_1(t)$), identify the iteration counter $n = 0$, iteration threshold σ (determined according to positioning accuracy) and the maximum iteration time N .

Step 2: Calculate the receiver position $x_r(t)$ through conventional nonlinear single-point positioning;

Step 3: Obtain the double-differenced pseudorange observations $D_m^T \cdot \tilde{p}_r^s(t)$;

Step 4: Compute the estimation of the unknown parameter, the relative distance between receiver r and reference receiver $\tilde{x}_{r_0}(t)$;

Step 5 (ESTIMATION): Calculate the LOS vector from the receiver $x_{r_0}(t)$ ($x_{r_0}(t)$ donates the estimation on the receiver position) to each transmitter and get the matrix $D_m^T \cdot G_r(t)$;

Step 6: Compute the nonlinear compensation $\epsilon_n(t)$ for each transmitter and the differenced compensation $D_m^T \cdot \epsilon_n(t)$;

Step 7: Approximate the unknown parameter $\tilde{x}_r(t)$ through least-squares principle;

Step 8: Calculate the difference between $\tilde{x}_r(t)$ and $\tilde{x}_{r_0}(t)$, and $n = n + 1$;

Step 9 (UPDATE): If $(\tilde{x}_r(t) - \tilde{x}_{r_0}(t) > \sigma | n > N)$ goto Step 4 and set $\tilde{x}_r(t) = \tilde{x}_{r_0}(t)$ else goto Step 10;

Step 10: Report $\tilde{x}_r(t)$.

The algorithm steps mentioned above can be expressed as the flow chart, as shown in Fig. 3 at the top of next page, where the $\tilde{x}_r(t) - \tilde{x}_{r_0}(t)$ defines the difference between estimated parameters in the last two iterations, the maximum number of iterations N within one epoch is set according to the system’s application scenarios.

2) ALGORITHM INNOVATIONS

The core idea of designing the PILSBON algorithm is described in a concentrated manner in this section. The key innovation of the proposed algorithm lies in the concept of using the specific characters of the problem as a priori knowledge. For the nonlinear error in the ground-based position determination, some pure nonlinear algorithms are capable of overcoming it [21]–[23], but the reason is that the algorithms are usually a complicated mixture of different aspects, which involve several complicated portions, like LM, UKF [9]–[11], [17], [18]. In the proposed algorithm, since the to-be-estimated parameter and the pseudorange decomposition method different from the conventional linearization positioning algorithm are employed, the nonlinear error caused by the linearization process is eliminated essentially by the nonlinear compensation term in the iterative process. Furthermore, the PILSBON algorithm based on the compensation is proposed where the linear least-squares method is

$$D_m^T \cdot \begin{bmatrix} p_r^1(t) - p_1^1(t) \\ \vdots \\ p_r^m(t) - p_1^m(t) \end{bmatrix} = [D_m^T \cdot G_r(t) \ I_{m-1}] \cdot \begin{bmatrix} \tilde{x}_r(t) \\ D_m^T \cdot \epsilon_n(t) \end{bmatrix} + e_{dd} \tag{16}$$

$$\begin{aligned}
 A_{11} &= \left(\frac{(y_r - y^s)^2 + (z_r - z^s)^2}{(\rho_r^s)^3} - \frac{(\rho_r^s)^2 (2(x_1 - x^s)(x_r - x^s) + \xi_s) - 3(x_r - x^s)^2 \xi_s}{(\rho_r^s)^5} \right) \\
 &\quad - \left(\frac{(y_r - y^p)^2 + (z_r - z^p)^2}{(\rho_r^p)^3} - \frac{(\rho_r^p)^2 (2(x_1 - x^p)(x_r - x^p) + \xi_p) - 3(x_r - x^p)^2 \xi_p}{(\rho_r^p)^5} \right) \\
 A_{22} &= \left(\frac{(x_r - x^s)^2 + (z_r - z^s)^2}{(\rho_r^s)^3} - \frac{(\rho_r^s)^2 (2(y_1 - y^s)(y_r - y^s) + \xi_s) - 3(y_r - y^s)^2 \xi_s}{(\rho_r^s)^5} \right) \\
 &\quad - \left(\frac{(x_r - x^p)^2 + (z_r - z^p)^2}{(\rho_r^p)^3} - \frac{(\rho_r^p)^2 (2(y_1 - y^p)(y_r - y^p) + \xi_p) - 3(y_r - y^p)^2 \xi_p}{(\rho_r^p)^5} \right) \\
 A_{33} &= \left(\frac{(y_r - y^s)^2 + (x_r - x^s)^2}{(\rho_r^s)^3} - \frac{(\rho_r^s)^2 (2(z_1 - z^s)(z_r - z^s) + \xi_s) - 3(z_r - z^s)^2 \xi_s}{(\rho_r^s)^5} \right) \\
 &\quad - \left(\frac{(y_r - y^p)^2 + (x_r - x^p)^2}{(\rho_r^p)^3} - \frac{(\rho_r^p)^2 (2(z_1 - z^p)(z_r - z^p) + \xi_p) - 3(z_r - z^p)^2 \xi_p}{(\rho_r^p)^5} \right) \tag{19} \\
 tr \left[\partial_{xx}^2 A_p(\tilde{x}_r(t)) \right] &= \frac{2\rho_r^s - \rho_1^s \left((e_1^s)^T \cdot e_r^s \right)}{(\rho_r^s)^2} - \frac{2\rho_r^p - \rho_1^p \left((e_1^p)^T \cdot e_r^p \right)}{(\rho_r^p)^2} \tag{20}
 \end{aligned}$$

employed for position determination. With the understanding of the origin of nonlinear error, the observable model can be transformed into a linear form which makes it not necessary to use those sufficiently robust but complicated ones. As a result, the nonlinear error can be corrected with a low calculation cost, leading to a balance between robustness and complexity. The application performance of the proposed algorithm is further evaluated by simulation.

The idea of improving the specificity and efficiency of the algorithm through involving prior knowledge can potentially be applied to other algorithmic applications in different fields, and is not limited to the field of localization algorithms in this paper.

C. PERFORMANCE ANALYSIS OF THE PILSBON ALGORITHM

Similar to the discussion in subsection II.C, the statistical characteristics of the PLSSBON algorithm should be performed. In this Section we mainly analyze the statistical properties of the PILSBON algorithm, referring to the research idea used by TEUNISSEN in [25] for the nonlinear least-squares method.

Due to the existence of nonlinear compensation, the proposed algorithm essentially adopts a linearization method, so it is necessary to analyze the residual deviation formed during the linearization process. In [25], the influence of nonlinearity is mainly evaluated based on the Hessian matrix of the measurement equation and the variance matrix of the numerical estimation algorithm. The Hessian matrix reflects the geometric characteristics of the system, while the variance matrix characterizes the estimate of the performance of the algorithm.

The equation for calculating the deviation due to nonlinearity can be expressed as follows:

$$b = -\frac{1}{2} tr \left[\partial_{xx}^2 A(x) Q(x) \right] \tag{17}$$

where $A(x)$ denotes the error equation of the system, $Q(x)$ is the variance matrix of the numerical estimation method (Linear least-squares method), $tr[\]$ means the trace of the matrix.

Based on the (17), the statistical evaluation of the PILSBON algorithm can be carried out. First, we consider the relationship between the double-differenced pseudorange model for a non-pivot transmitter s and the receiver's position, which is shown in (13). At the same time, because the numerical estimation method in the proposed algorithm is the traditional linear least-square estimation method, the $Q(x)$ is defined as $Q(x) = \sigma_x^2 I$.

The Hessian matrix for (13) is calculated first, which can be expressed as follows:

$$\partial_{xx}^2 A_p(\tilde{x}_r(t)) = \begin{bmatrix} A_{11} & & \\ & A_{22} & \\ & & A_{33} \end{bmatrix} \tag{18}$$

Since the final bias resolution only requires the trace of the Hessian matrix, only three values on the trace are listed as (19), shown at the top of this page. Thereinto $\xi_s = (x_1 - x^s)(x_r - x^s) + (y_1 - y^s)(y_r - y^s) + (z_1 - z^s)(z_r - z^s)$ and $\xi_p = (x_1 - x^p)(x_r - x^p) + (y_1 - y^p)(y_r - y^p) + (z_1 - z^p)(z_r - z^p)$.

Then we can find the trace of the Hessian matrix as (20), as shown at the top of this page.

According to (20), the deviation b due to linearization in the algorithm is finally obtained.

$$b = \sigma_x^2 \left(\frac{\rho_r^p - \frac{1}{2} \rho_1^p \left((e_1^p)^T \cdot e_r^p \right)}{(\rho_r^p)^2} - \frac{\rho_r^s - \frac{1}{2} \rho_1^s \left((e_1^s)^T \cdot e_r^s \right)}{(\rho_r^s)^2} \right) \quad (21)$$

According to (21), the deviation due to nonlinearity is related to the position of the reference receiver and the transmitters, and also to the deviation of the estimator. The Equation (21) is equivalent to subtracting a part (related to nonlinear compensation) from the deviation of the traditional least squares algorithm. The PLSBON algorithm's capability of reducing the nonlinear effect is also proved by the above formula. At the same time, it can be found that as the system launched in a smaller area, this deviation also shows a downward trend. For example, in the satellite application environment, (21) is also negligible.

In order to overcome the nonlinear error, the nonlinear compensation and the PILSBON algorithm are proposed in this Section. The statistical properties of the algorithm are also analyzed and illustrated in Subsection III.C. Through the analysis, there is a possibility that the proposed algorithm is able to achieve robust position determination in the presence of strong nonlinearity with moderate accuracy. The results of both simulations and the experiments will be shown in the next Section.

IV. SIMULATION AND EXPERIMENTAL DATA RESULTS

In this Section, the two specific scenarios depending on knowledge of the position of the reference receiver are described. Then, the results of both theoretical simulations and real data experiments based on a practical ground-based positioning system are presented. Our attention is mainly focused on the robustness of the performance, which is represented by the bias of the position estimation.

A. ABSOLUTE POSITIONING AND RELATIVE POSITIONING

In this Subsection, two specific scenarios of the system are described, namely the absolute and relative positioning. The significance of discussing these two application scenarios lies in the following two points. First, in actual system applications, the reference receiver is not necessarily accurate due to environmental influences and equipment shortages, or the position accuracy cannot meet the system positioning accuracy requirements. The enumeration of cases under different application conditions improves our analysis of the algorithm. Second, the importance of the precise position of the reference receiver for system positioning performance can be further illustrated by comparison with the context in which the reference receiver position is accurately known.

The definitions of these two scenarios are the following.

- *Absolute Positioning*

When the reference receiver is located in a known position, the distance term mentioned above is obtained precisely. This precisely known position can be sourced

from two sources. First, it can be measured by a total station or other positioning means along with all the transmitters in the actual test. The total station can provide measurement results in the accuracy of millimeters, while for the other, the accuracy is determined according to the specialty of the method; secondly, the reference receiver can be placed on a target that is precisely known at a certain position (such as latitude and longitude), for example, a satellite signal forwarding station. In this situation, the estimation of the receiver position refers to the absolute position in the coordinate system of the working area.

- *Relative Positioning*

When the accurate position of the reference receiver is unavailable, the pseudorange obtained by the reference receiver is used as an alternative to forming the nonlinear compensation. In contrast to (15), compensation is defined as

$$\varepsilon_n(t) = \begin{bmatrix} p_1^1(t) \cdot (1 - e_1^1(t)^T \cdot e_r^1(t)) \\ \vdots \\ p_1^m(t) \cdot (1 - e_1^m(t)^T \cdot e_r^m(t)) \end{bmatrix} \quad (22)$$

Therefore, the final estimation of the receiver is actually the relative position referenced to the estimated reference receiver, maybe from single-point positioning. There is no doubt that compensation involving several error terms caused by pseudorange will lead to a contaminated positioning result.

B. SIMULATION RESULTS

1) SCENE SETTINGS

The simulation was built in MATLAB for the analysis of robustness in the specific nonlinearity environment. It is necessary to describe the settings of the simulations in this part before the results are shown.

In the conventional system structure, in order to emphasize the reference role of the reference receiver, the reference receiver was generally placed at a position closer to the center of the coverage area of the system. To verify the performance of different methods in each epoch when faced with increasing nonlinear errors, the receiver was requested to move from the center of the system coverage, which was located near the reference receiver, to a position close to a certain transmitter. Throughout the motion trajectory, the nonlinearity was increasing. As a result, the difficulty of position determination would increase significantly.

The entire simulation system consists of five transmitters and two receivers, where the receiver used as the reference remains stationary and the other receiver acts as a rover to move according to a particular trajectory. Five transmitters were assumed and located on the boundary of an area which was 100 m x 100 m x 10 m. The assumed structure of the ground-based positioning system is shown in Fig. 4.

In this paper, parameters to be estimated are only three-dimensional receiver coordinates because of the

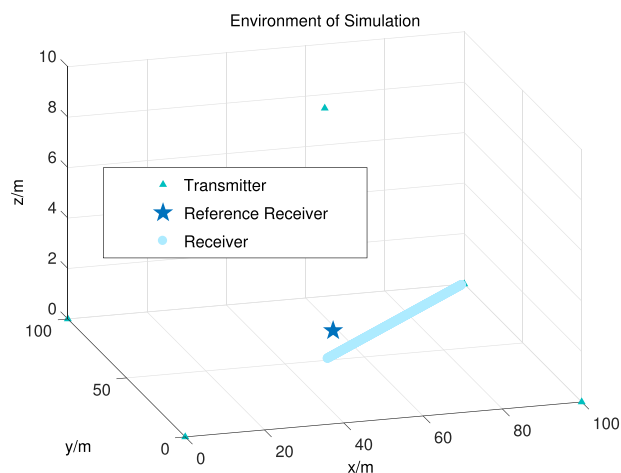


FIGURE 4. Location of devices, with five ground-based transmitters, a static reference receiver, and a kinetic receiver.

double-differenced model, so the minimum required number of transmitters is 3. However, if a single point positioning is required before double-differenced positioning to obtain an initial value with a certain confidence, at least 4 transmitters are needed to satisfy the further estimation of the unknown receiver clock bias. In the simulation, we consider the three factors of trade-off, information redundancy, calculation complexity, and signal source geometric distribution. Finally, we choose to set the simulation scenario to be like Fig. 4. The system Dilution of Precision (DOP) value in this scenario is shown in Fig. 5.

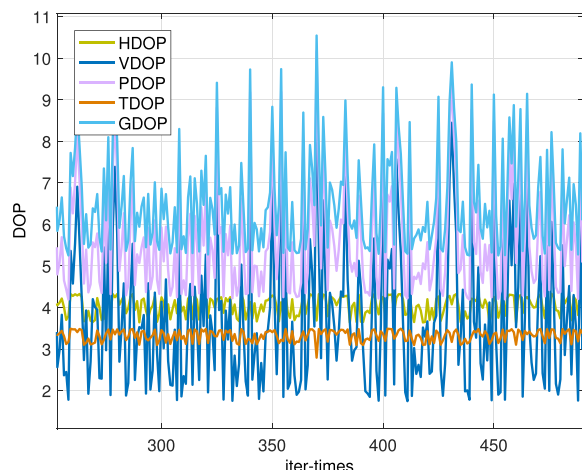


FIGURE 5. DOP value in the context of the simulation experiment.

The situation in Fig. 5 is the change in the system’s DOP value as the simulation proceeds. It can be seen from the figure that the GDOP value is stable within 10, indicating that the influence of measurement error on the positioning result will be limited.

We also give an overall description of the error parameters used in the simulation. In all simulations, the true pseudoranges were contaminated with Gaussian noise of zero

mean and a standard deviation of 10 cm. Based on the definition of Gaussian noise, it could be estimated that the Root Mean Square (RMS) error of the positioning result with double-difference model would be at this level. Along with the Gaussian noise, the measurements also contained the synchronization bias of both the transmitters and the receivers. Based on the realistic conditions of the system, the synchronization bias of the transmitters was set to vary from -15 ns to 15 ns for every epoch, while that of the receiver varied from 35 ns to 45 ns.

During the rendering of the simulation results, to demonstrate the performance of the PILSBON algorithm compared with other conventional methods, a specific metric is needed. Given that the true position of the receiver is known as prior information, the RMS error is employed. In each simulation, the motion trajectory of the receiver consists of 500 points, and the data received by the receiver at each point conform to the above signal parameter settings. The algorithm used to perform the performance comparison processes the same data in order to control the variables. Additionally, in order to verify the need of the algorithm for accurate initial estimations, a random initial error is added to the position determination of each epoch. The added error is decided according to the size of the simulation court. The error for the simulations mentioned above, for example, is set to be a random error with a standard deviation of 20 meters.

For the following simulations, the scenarios for both absolute and relative positioning are demonstrated in two specific parts.

2) SIMULATION WITH PILSBON ALGORITHM FOR THE RELATIVE POSITIONING SCENARIO

The purpose of the first simulations, which were carried out in relative positioning, was to demonstrate the performance of the proposed algorithm for coping with the nonlinear error.

To prove the necessity of the nonlinear compensation, typical iterative least-squares estimation (LSE) and PILSBON algorithms were chosen for comparison in the simulation.

Fig. 6 plots the RMSE of the algorithms involved in every epoch. The figure can be divided into three parts according to the motion of the receiver. For the beginning of the receiver motion, iterative LSE is able to achieve position determination with expected accuracy. Nevertheless, when the receiver moves to a position which is far from the reference receiver and the distance from a transmitter is gradually reduced, the divergence can be observed immediately for the iterative LSE method according to (8), which refers to the scenarios after 120 epochs. Errors around 20 meters are observed near the 100 epochs, showing drastic fluctuations, which is the result of the nonlinear error. In this situation, the estimation of the unknown parameter, together with that of the differenced pseudorange is diverging in a wrong direction. The second part is the middle section of the movement (120-400 epoch). It is now impossible for LSE method to obtain a convergent solution for the position determination. However, thanks to the nonlinear compensation, the PILSBON algorithm shows

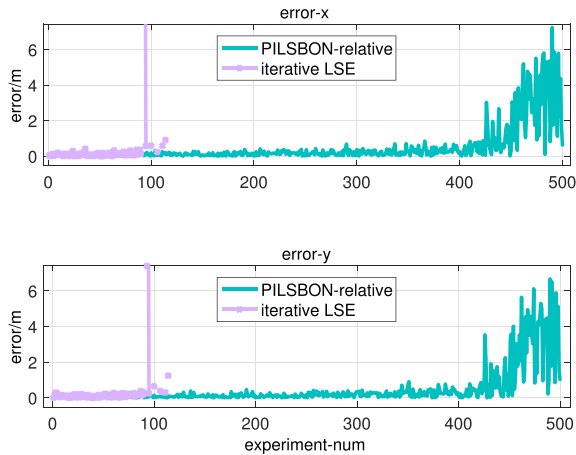


FIGURE 6. RMS error of the positioning results from conventional iterative LSE and PILSBON in relative positioning; 500 epochs are considered for the comparison.

noticeably better performance than that of the iterative LSE during almost the entire motion.

However, for the final part of the motion (after 400 epoch), the effect of the nonlinear error on PILSBON is clearly seen and leads to a distinct increase in the RMS error. We anticipated this result, which was discussed in the description of relative positioning in Section IV.A. The magnitude of the observational pseudorange error and the observation itself become comparable with the motion of the receiver towards a transmitter. This leads the effect caused by the error from the pseudorange observation to become so severe that it cannot be ignored, causing fluctuating positioning results.

In the next part, we consider the absolute positioning, where the reference receiver is located in a precisely known position, which means there is no reference-related error term involved in the nonlinear compensation. There is no need to proceed to a single-point position determination for the reference receiver which leads to an accurately calculated compensation.

3) SIMULATION ON PILSBON ALGORITHM FOR THE ABSOLUTE POSITIONING SCENARIO

The results presented so far confirm the applicability of PILSBON for strong nonlinearity. However, in the application condition of absolute positioning, the accuracy of the nonlinear compensation is predicted to be further improved due to the better positional accuracy of the reference receiver.

The reference receiver is still placed at the corresponding coordinates above, the difference is that this position is considered as a precisely known information. As a matter of fact, the reference receiver can be situated in any position with accurate coordinates, which utilized here are only a specific example. Other settings for the simulations remain unchanged.

The improvement in accuracy in absolute positioning scenario can be seen clearly in Fig. 7. Since the position of the reference receiver is accurate, the calculation of the nonlinear

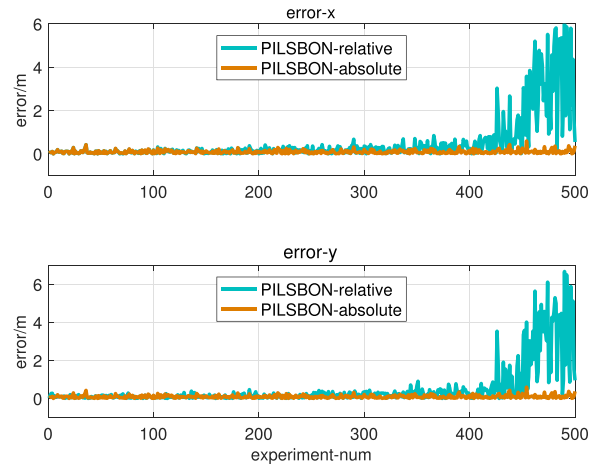


FIGURE 7. RMS error of the positioning results from PILSBON in both absolute and relative positioning, 500 epochs are considered for the comparison.

compensation is not be affected by the measurement error as above. It can be seen from the figure that the RMS error distribution of relative positioning shows enormous fluctuation in the final part of the motion relative positioning scenario, but there is not clear deterioration in the same part of the motion in the absolute positioning scenario.

So far, we found that PILSBON can effectively suppress nonlinear errors under the premise that the reference receiver information is accurately known. However, considering that the nonlinear methods such as the LM algorithm are also widely used in the numerical estimation of the positioning algorithm, we perform an additional comparative simulation to further evaluate the performance of the PILSBON algorithm. This simulation shares with the same simulative scenario as before, the results of which are shown in Fig. 8.

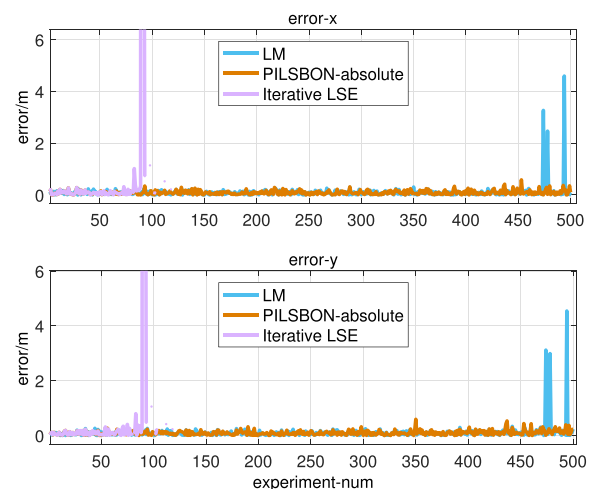


FIGURE 8. Performance comparison between PILSBON algorithm, traditional iterative LSE and nonlinear LM algorithm.

In the figure, we find that the LSE algorithm still shows rapid error growth at the starting part of the trajectory.

The LM algorithm used for comparison is obviously capable of the positioning application in the above nonlinear situation as a standard nonlinear algorithm. But when the nonlinearity is very strong, several errors appear in the estimated result of the LM algorithm. In terms of suppressing nonlinear errors, the PILSBON algorithm exhibits greater pertinence and specificity.

To summarize, the results of the simulations described in Subsection IV.B provide evidence of the negative effect caused by the nonlinear error on ground-based positioning applications, together with the capability of the nonlinear compensation to overcoming it. The PILSBON algorithm is able to achieve position determination with moderate accuracy, while not demanding a precise initial estimation. Furthermore, the simulations corresponding to the relative and absolute positioning scenarios demonstrate the benefit of a known reference receiver position (Subsection IV.B.2). Moreover, traditional nonlinear positioning methods represented by LM is introduced as a comparison, the superiority of the PILSBON algorithm on solving the nonlinear error is further explained (Subsection IV.B.3).

In the next Subsection, we use experiments based on a practical ground-based transmitter system to further demonstrate the performance superiority of the proposed algorithm.

C. EXPERIMENTAL DATA RESULTS

In the previous Sections, the simulations on the PLSSBON algorithm illustrate the capability of the algorithm to overcome nonlinear effects. To further illustrate algorithm performance in practical applications, we need to perform experiments in the actual regional positioning system. In this Section, the installation hardware of the ground-based positioning system is first presented before exposing the results of the experiments conducted with it.

1) EXPERIMENTAL SETTINGS AND GROUND-BASED POSITIONING SYSTEM

Experimental data was obtained through an open-area positioning system situated on the rooftop of the Weiqing building on the campus of Tsinghua University. The system consists of six ground-based signal transmitters and one receiver. The PILSBON algorithm proposed is used to process the signals of the practical ground-based regional positioning system. The positioning results are plotted by Matlab and the performance analysis is performed.

In positioning systems, the number of signal sources is flexible in order to achieve different positioning requirements. As mentioned in section IV.B, the number of transmitters should be no less than four. Generally speaking, an increase in the number of visible signal sources leads to an increase in positioning accuracy, mainly due to increased data redundancy and better signal source geometry. However, the increase in the number of signal sources also causes an increase in the calculation complexity of the algorithm, so it is necessary to find a balance between complexity and positioning accuracy. The corresponding study on the optimization

can be found in [26] and [27]. In the experiments herein, the number of transmitters is selected to be six, with the actual experimental site environment involved, and the two factors mentioned above considered comprehensively.

The whole system is launched based on a software platform. Each signal transmitter is made of three components: the mainframe, radio frequency channel and antennas for the reception and transmission of signals. The ranging signals are generated with an intermediate frequency of 46.43 MHz and used to modulate a 2.4GHz carrier frequency. The up and down-conversion of frequency and conversion between digital and analog signals are achieved within the RF channel device. The transmitters in the ground-based positioning system are actually transceivers which are able to serve as both transmitters and receivers. The two antennas shown in the left half of Fig. 9 are used to transmit and receive signals respectively.



FIGURE 9. Experimental environments and devices employed.

The antennas are connected with the RF channel device through SMA cabling. The experimental environment and deployment of the necessary devices are displayed in Fig. 9. The antenna attached with the mobile receiver is located on a remote-controlled wheeled mobile robot, which moves along a specific trajectory according to the experiment scenarios. In order to strengthen the stability of the ground-based transmitter antennas, environmental structures like walls and specially-made columns are used to provide support, also shown in Fig. 9. The support for the antennas is required to provide sufficient stability even in windy weather. All experiments mentioned in this subsection were carried out within this venue.

The time synchronization of the system used is mainly based on selecting a transmitter as the master information source. The specific process used is that the master

transmitter transmits the reference positioning signal to other slave transmitters, and those slave transmitters then send back a positioning signal to other transmitters. Time synchronization is achieved by steps of time coarse alignment, frequency lock, code lock, and phase lock. The detailed time synchronization algorithm can be found in [24].

Each transmitter has the function of sending and receiving signals at the same time, double-differenced pseudorange observations between receivers were obtained through selecting a specific transmitter as the reference receiver. The reference receiver (transceiver) for experiments shown in this subsection was set to be the transmitter labeled 1. It is also the master transmitter in the transmitter network. The schematic diagram of the whole system is shown in Fig. 10.

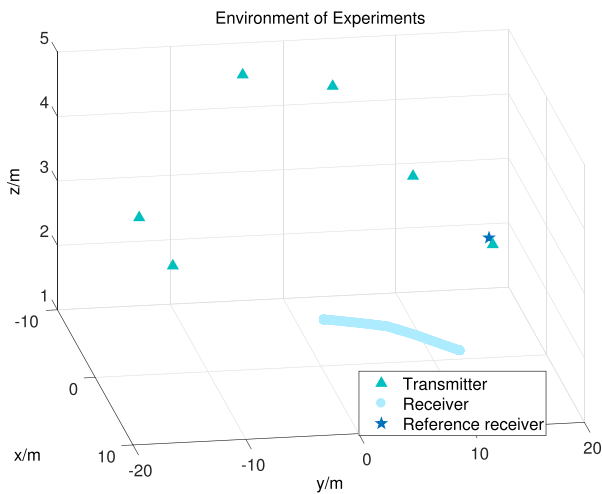


FIGURE 10. Schematic diagram of experimental environments and devices employment.

Unlike the scenario in the simulations, the transmitter position used in the field experiment were measured by the total station before the experiment. The accuracy of total station measurement used in this experiment is on the order of millimeters. As a result, the reference receiver position can be considered accurate and remains unchanged during the experiment. Therefore the absolute positioning scenario is deployed in all experiments. The actual positioning result used in the experiment is based on the carrier phase positioning results obtained in advance by getting the accurate integer ambiguity [6]. The final positioning accuracy of the real positioning results is on the order of centimeter (according to previous field experiment experience, usually about 2-3cm).

Regarding the motion trajectory of the receiver in figure 12, a similar scenario as the simulation was set for the proposed algorithm to certify the ability of position determination in strong nonlinearity. During the motion, the receiver continuously receives the pseudorange information, and the obtained signal is input into the PILSBON algorithm for positioning.

Next, it is necessary to evaluate the environment of the experimental system and the signal source geometric distribution. Referring to the analysis in the simulations in IV.B.1, the change of the DOP together with the receiver motion in

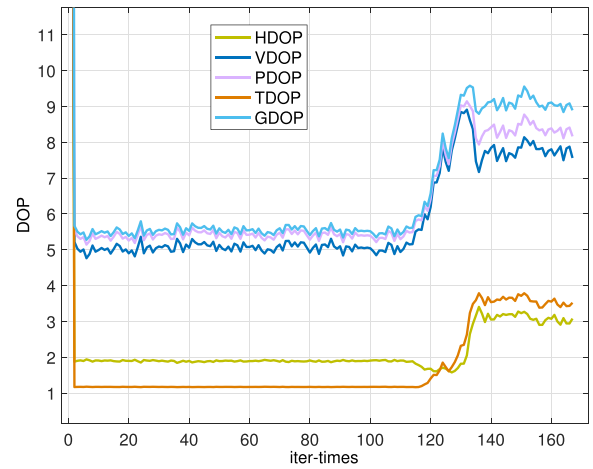


FIGURE 11. Change of DOP value under experimental data situation.

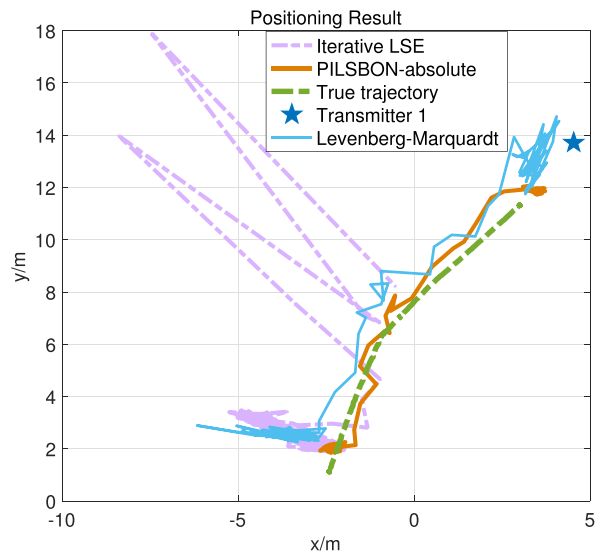


FIGURE 12. Scatter diagram of position determination results obtained with iterative LSE, LM, and PILSBON in absolute positioning, with the comparison to true positions.

the experimental context is illustrated here. The specific DOP is shown in Fig. 11.

It can be seen that due to the increase in the number of receivers, the previous period of the DOP value is relatively lower and the value is more stable. However, there is a significant improvement in the latter part of the motion. This is because the receiver has gradually moved closer to transmitter No. 1 (beginning from about the 110th experiment). Finally, since the receiver is completely stable near the base station, the DOP value continues to be higher. The overall DOP value is always stable below 10, which means that increasing the number of signal transmitters and improving the distribution of them can indeed reduce the influence of measurement errors to some extent.

Due to the limitation of the rooftop site, the system is currently only applied to the regional positioning situation of the site with a dimension of about 20m. In order to adapt to the existing coverage, the signal is set at 10mW for RF transmit power to ensure that the power meets the working requirements of the system. As the system is used in the

expected range (km-level) application environment, the signal transmission power will be correspondingly improved.

Additionally, similar to the simulations, a random error with a standard deviation of 15 meters is added to the true position and regarded as the initial estimation. The adaptive ability to undesirable initial accuracy is verified by doing this. The results of the experiments are shown in the next part.

2) EXPERIMENT RESULTS

The experiments results in the scenarios described above are presented in this part. It has been demonstrated in Section IV.C.1 that only the absolute scenario is used in the experiments.

In order to compare the performance of selected algorithms, the experiment involves the position determination results of iterative LSE, LM algorithm and PILSBON algorithm and compares them with the real motion trajectory of the receiver.

The scatter plot of the positioning results of each positioning algorithm is shown in Fig. 12.

According to Fig. 12, the most striking characteristic we observe is the significant difference in the position determination trajectories obtained through use of the iterative LSE and PILSBON algorithm. We can also see in Fig. 8 that the simulative performance of the iterative LSE is similar to its performance in experiments. In comparison, the PILSBON in absolute positioning shows a trajectory that fits the true motion well. In addition, compared with the standard nonlinear method LM algorithm, the positioning results show that both LM and PILSBON can match the motion trajectory of the receiver. However, when the nonlinearity is strong, the fluctuations on the LM algorithm's positioning results appeared as predicted in simulations compared to the better convergence and stability of PILSBON algorithm. Comprehensively speaking, from the results shown in Fig. 12, PILSBON achieves better performance overall compared to the iterative LSE and LM algorithm.

However, whether it is the LM algorithm or the PILSBON algorithm, compared with the simulation results in Section IV.B.

Among the sources of error that may have a large impact, there are two main components regardless of the measurement error. One is the influence of nonlinear error, and the other is the effect of the multipath effect. These two effects widely exist in the positioning system, but the influence of both is particularly obvious in the ground-based positioning system.

First consider the influence of the nonlinear effects, which can be analyzed by the difference between the estimates of the double-differenced pseudoranges and the measured values in the iterative numerical solution process. In order to show more clearly the significance of the nonlinear compensation in numerical estimation, the double-differenced pseudorange observation and the estimation are performed both with and without nonlinear compensation. The comparison based on experiments is shown in Fig. 13.

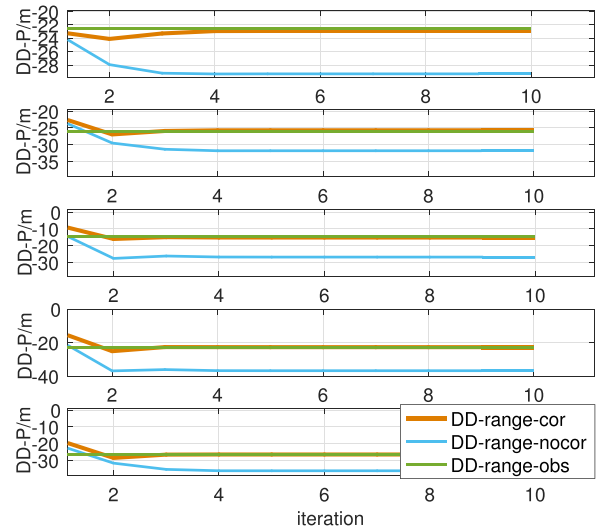


FIGURE 13. The comparison between the estimation and the observation of the double-differenced pseudorange between each transmitter and the pivot transmitter in the least-squares estimation. Both the pseudorange estimation with compensation and without compensation are shown.

Each sub-figure in Fig. 13 refers to a transmitter, which corresponds to 5 double-differenced observations obtained from 6 transmitters. The iteration of the estimation step in an epoch is shown, both the pseudorange with and without compensation are considered.

These results show that the estimation of the double-differenced pseudorange will converge to the observation rapidly if the nonlinear compensation is involved (red line), while the estimation without the compensation (blue line) will level off on a value with a gap from the true observation. The double-differenced pseudorange without compensation is obtained by removing the nonlinear compensation from the corrected one (red line). The reason is that, as has been shown above in the application of iterative LSE, it is impossible to achieve a convergent solution without the help of the compensation. Succinctly, the existence of the nonlinear compensation makes it possible for the algorithm to converge in the right direction.

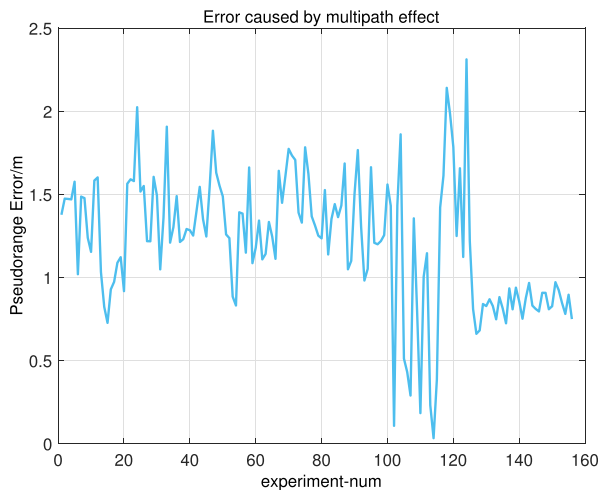
So far, it has been demonstrated that the nonlinear error is effectively eliminated in the proposed algorithm. Therefore, the main reason for the impact on positioning performance should be the multipath effect.

The existence of multipath effect in the ground-based positioning is mostly due to the complicated environment. Referring to the scenario shown in Fig. 9, the existence of significant blocking and reflection of signals leads to serious multipath effects, which minimize the benefit brought by the double-differenced technique. Given the employment of the double-differenced technique, clock bias from both transmitter and receivers was eliminated and would not lead to a significant negative impact, and neither would the measuring error according to the DOP. It should be mentioned that the multipath effects on the pseudorange come in the form of specific biases, which would be amplified or even doubled through the differential process. As a result, the position results obtained using the double-differenced model would

TABLE 1. Comparison of statistical results of positioning error in the simulation experiment and actual test.

Test type	LSE-Simulation	PILSBON-Relative-Simulation	LM-Simulation	PILSBON-absolute-Simulation	LSE-Experiment	LM-Experiment	PILSBON-absolute-Experiment
RMSE/m	2.8384	1.6979	0.3266	0.1740	4.7643	0.9778	0.6602
SD/m	1.4856	1.5292	0.2915	0.0904	2.8352	0.7965	0.3125

be even worse when compared to the single-point positioning method. In order to further analyze the influence of multipath effects, the difference between the pseudorange measurement and the real value is analyzed here. The pseudorange real value is calculated by the exact position of the receiver and the exact position of the transmitter. The difference between the pseudorange measurement and the true value is shown in Fig. 14.

**FIGURE 14. The difference between the pseudorange of transmitter number 2 and the true pseudorange obtained by the receiver.**

According to the information in figure 16, we find that during the whole movement, there is a large gap between the measured value and the true value, and the maximum point is even more than 2 meters, which obviously should not be the impact of measurement errors. Due to the size of the experimental site, the pseudorange measurement value does not exceed 20 meters at most, so the error shown in the figure is sufficient to have a serious influence on the positioning result. This directly causes the phenomenon that the positioning result in Fig. 12 deviates from the true motion trajectory.

Although there is a deviation, the PILSBON algorithm achieves the performance expectations in terms of specifically overcoming nonlinear errors and positioning stability. The capability of PILSBON to overcome the nonlinear error with moderate robustness is proved through the results of both simulations and experiments. Furthermore, it is not necessary to provide an accurate initial estimation of the unknown parameter unlike in most conventional nonlinear methods. Moreover, we carried out an individual experiment to verify the importance of nonlinear compensation in the PILSBON algorithm and the impact of multipath effects on positioning accuracy.

Finally, considering the importance of quantitative analysis for judging the performance of the algorithm, the statistical

results of the positioning results of the above simulations and experiments are collectively shown in Table 1.

Since the LSE algorithm fails in the middle of the receiver track, only the part in which the positioning result is valid can be counted. We find that although the measured results have a significant decline compared to the simulation results, they still show obvious advantages over the classic LSE algorithm. Moreover, the differences in the application scenarios of relative and absolute as discussed in Section IV.B.3 above are also evident in the table. In addition, the simulation results corresponding to the LM algorithm are added, which presents a certain probability of positioning error improvement. This phenomenon is shown in the positioning results in Sections IV.B.3 and IV.C.2.

V. CONCLUSIONS

In this paper, a method termed Promoted Iterative Least-Squares Based On Nonlinear-compensation (PILSBON) for position determination in ground-based positioning systems is presented to alleviate the error caused by nonlinearity. The proposed algorithm exploits a specific nonlinear compensation, the numerical expression of which is derived in this paper. The statistic properties of the proposed algorithm were also evaluated. Furthermore, the positioning process can be achieved using a linear least-squares method, and a highly precise initial estimation is not necessary. The PILSBON algorithm is carried out in two scenarios, namely the absolute positioning and relative positioning, where the performance is slightly affected by the accuracy of the reference receiver coordinates.

The PILSBON algorithm's efficiency and robustness in coping with the nonlinear error are evaluated and verified using simulations and experiments. The advantage of the PILSBON algorithm over the traditional algorithms is that it can provide stable positioning services with stable accuracy when the traditional algorithm (LSE) fails to locate strong nonlinear effects. According to the quantitative error results, we find that compared with the traditional algorithm without a specific solution to the nonlinear influence, the proposed algorithm can bring 30% of the RMS error under the experimental conditions 50% drop for simulations.

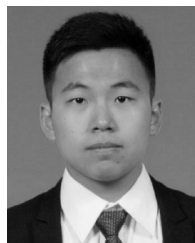
Furthermore, the idea of obtaining specific solutions using the inherent characters of the problems as known knowledge is implemented in this paper. The computational complexity of algorithms such as LM may not be high, even sometimes lower than the complexity of some specialized algorithms, but the essential reason is that the framework and flow of the algorithm itself have made it robust enough to be a universal and standard algorithm. However, with strong nonlinear effects mentioned in this paper, the advantages of the specialized algorithm are more obvious. The main reason for that

is that the error-related factors are eliminated essentially, as opposed to using a powerful and robust mathematical process.

Additionally, this idea of using prior knowledge and practical application scenarios can be widely applied in practical engineering applications to improve solving efficiency and serviceability.

REFERENCES

- [1] E. D. Kaplan and C. Hegarty, *Understanding GPS: Principles and Applications*. Norwood, MA, USA: Artech House, 2005.
- [2] J. Wang, T. Tsujii, C. Rizos, L. Dai, and M. Moore, "Integrating GPS and pseudolite signals for position and attitude determination: Theoretical analysis and experiment results," in *Proc. Int. Tech. Meeting Satell. Division Inst. Navigat.*, 2000, pp. 2252–2262.
- [3] J. Yan, C. C. J. M. Tiberius, G. J. M. Janssen, P. J. G. Teunissen, and G. Bellusci, "Review of range-based positioning algorithms," *IEEE Aerosp. Electron. Syst. Mag.*, vol. 28, no. 8, pp. 2–27, Aug. 2013.
- [4] E. A. Lemaster, "Self-calibrating pseudolite arrays: Theory and experiment," Ph.D. dissertation, Stanford Univ., Stanford, CA, USA, 2002.
- [5] W. Jiang, Y. Li, and C. Rizos, *Locata-Based Precise Point Positioning for Kinematic Maritime Applications*. New York, NY, USA: Springer-Verlag, 2015.
- [6] J. Barnes, C. Rizos, M. Kanli, and A. Pahwa, "A positioning technology for classically difficult GNSS environments from Locata," in *Proc. IEEE/ION Position, Location, Navigat. Symp.*, Apr. 2006, pp. 715–721.
- [7] T. Takasu, "Real-time PPP with RTKLIB and IGS real-time satellite orbit and clock," in *Proc. IGS Workshop*, 2010, p. 216.
- [8] L. Dai, J. Wang, T. Tsujii, and C. Rizos, "Pseudolite applications in positioning and navigation: Modelling and geometric analysis," in *Proc. Int. Symp. Kinematic Syst. Geodesy, Geomatics Navigat.*, 2001, pp. 482–489.
- [9] J. Yan, C. Tiberius, G. Bellusci, and G. Janssen, "Feasibility of Gauss-Newton method for indoor positioning," in *Proc. IEEE/ION Position, Location Navigat. Symp.*, May 2008, pp. 660–670.
- [10] S. Zhao, Z. Yao, J. Yin, and M. Lu, "Application of extended and unscented Kalman filtering for non-linear positioning in nearby region of navigation sources," in *Proc. Inst. Navigat. Int. Tech. Meeting (ITM)*, Jan. 2015, pp. 640–650.
- [11] X. Li, P. Zhang, J. Guo, J. Wang, and W. Qiu, "A new method for single-epoch ambiguity resolution with indoor pseudolite positioning," *Sensors*, vol. 17, no. 4, p. 921, 2017.
- [12] S. Zhao, X. Cui, F. Guan, and M. Lu, "A Kalman filter-based short baseline RTK algorithm for single-frequency combination of GPS and BDS," *Sensors*, vol. 14, no. 8, pp. 15415–15433, 2014.
- [13] X. G. Wan, X. Q. Zhan, and G. Du, "Carrier phase method for indoor pseudolite positioning system," *Appl. Mech. Mater.*, vols. 130–134, no. 37 pp. 2064–2067, 2012.
- [14] J. J. Liang, A. K. Qin, P. N. Suganthan, and S. Baskar, "Comprehensive learning particle swarm optimizer for global optimization of multimodal functions," *IEEE Trans. Evol. Comput.*, vol. 10, no. 3, pp. 281–295, Jun. 2006.
- [15] F. van den Bergh and A. P. Engelbrecht, *A Study of Particle Swarm Optimization Particle Trajectories*. Amsterdam, The Netherlands: Elsevier, 2006.
- [16] C. De Marziani et al., "Relative localization and mapping combining multidimensional scaling and levenberg-marquardt optimization," in *Proc. 6th IEEE Int. Symp. Intell. Signal Process.*, Aug. 2009, pp. 43–47.
- [17] M. Sivers and G. Fokin, "LTE positioning accuracy performance evaluation," *Internet of Things, Smart Spaces, and Next Generation Networks and Systems*. Cham, Switzerland: Springer, 2015, pp. 393–406. doi: 10.1007/978-3-319-23126-6_35.
- [18] R. Babu and J. Wang, "Ultra-tight integration of pseudolites with INS," in *Proc. IEEE/ION Position, Location, Navigat. Symp.*, Apr. 2006, pp. 705–714.
- [19] P. J. G. Teunissen and O. Montenbruck, *Springer Handbook of Global Navigation Satellite Systems*. Cham, Switzerland: Springer, 2017. doi: 10.1007/978-3-319-42928-1.
- [20] F. U. Guangren, Z. Cao, M. I. Linshan, and D. Sun, "Pseudolite positioning algorithm based on least squares and EKF," *Comput. Eng. Appl.*, vol. 48, no. 34, pp. 148–151, 2012.
- [21] K. Fujii, R. Yonezawa, Y. Sakamoto, A. Schmitz, and S. Sugano, "A combined approach of Doppler and carrier-based hyperbolic positioning with a multi-channel GPS-pseudolite for indoor localization of robots," in *Proc. IEEE Int. Conf. Indoor Positioning Indoor Navigat.*, Alcalá de Henares, Spain, Oct. 2016, pp. 1–7. doi: 10.1109/IPIN.2016.7743668.
- [22] N. Samama, A. Vervisch-Picois, and T. Taillandier-Loize, "A GNSS-based inverted radar for carrier phase absolute indoor positioning purposes first experimental results with GPS signals," in *Proc. Int. Conf. Indoor Positioning Indoor Navigat.*, Oct. 2016, pp. 1–8.
- [23] J. Wang et al., "Synchronisation method for pulsed pseudolite positioning signal under the pulse scheme without slot-permutation," *IET Radar, Sonar Navigat.*, vol. 11, no. 12, pp. 1822–1830, 2017.
- [24] T. Wang, Z. Yao, S. Yun, and M. Lu, "A new network-based synchronization approach for pseudolite and improvements on robustness," in *Proc. 29th Int. Tech. Meeting Satell. Division Inst. Navigat. (ION GNSS)*, Portland, OR, USA, Sep. 2016, pp. 838–844.
- [25] P. J. G. Teunissen, "First and second moments of non-linear least-squares estimators," *Bulletin Géodésique*, vol. 63, no. 3, pp. 253–262, 1989.
- [26] F. Ellinger et al., "Local positioning for wireless sensor networks," in *Proc. IEEE Globecom Workshops*, Nov. 2008, pp. 1–6.
- [27] P. Mäkelä, "Local positioning systems and indoor navigation," M.S. thesis, Tampere Univ. Technol., Tampere, Finland, 2008.
- [28] X. Gan, B. Yu, Z. Heng, L. Huang, and Y. Li, "Indoor combination positioning technology of Pseudolites and PDR," in *Proc. Ubiquitous Positioning, Indoor Navigat. Location-Based Services (UPINLBS)*, Wuhan, China, Mar. 2018, pp. 1–7.
- [29] R. Zhu, X. Gan, Y. Li, H. Zhang, S. Li, and L. Huang, "An indoor location method based on optimal DOP of displacement vector components and weighting factor adjustment with multiple array pseudolites," in *Proc. Ubiquitous Positioning, Indoor Navigat. Location-Based Services (UPINLBS)*, Wuhan, China, Mar. 2018, pp. 1–7.
- [30] J. Gehrt, M. Breuer, T. Konrad, and D. Abel, "A pseudolite position solution within a Galileo test environment for automated vehicle applications," in *Proc. Eur. Navigat. Conf. (ENC)*, Lausanne, Switzerland, May 2017, pp. 135–142.



JINGXUAN SU received the B.E. degree from Tsinghua University, in 2016, where he is currently pursuing the master's degree with the Department of Electronic Engineering. His research interest includes pseudolite system development and signal analyzing.



ZHENG YAO received the B.E. degree in electronics information engineering and the Ph.D. degree Hons. in information and communication engineering from Tsinghua University, Beijing, China, in 2005 and 2010, respectively, where he is currently an Associate Professor with the Department of Electronic Engineering. His current research interests mainly include next-generation satellite navigation signals design, software-defined receiver, new location technologies, and personal and vehicular positioning in challenging environments. He was a recipient of the 2017 Early Achievement Award and the 2008 Student Paper Award from the U.S. Institute of Navigation.



MINGQUAN LU received the M.E. and Ph.D. degrees in electronic engineering from the University of Electronic Science and Technology, Chengdu, China. He is currently a Professor with the Department of Electronic Engineering, Tsinghua University. His research interests include wireless networks, satellite communication and navigation, and signal processing.